
Discovery and initial characterization of YloC, a novel endoribonuclease in *Bacillus subtilis*

SHAKTI INGLE,¹ SHIVANI CHHABRA,¹ JIANDONG CHEN,² MICHAEL B. LAZARUS,¹ XING LUO,³ and DAVID H. BECHHOFFER¹

¹Department of Pharmacology and Systems Therapeutics, Icahn School of Medicine at Mount Sinai, New York, New York 10029, USA

²Department of Microbiology, Perelman School of Medicine, University of Pennsylvania, Philadelphia, Pennsylvania 19104, USA

³Laboratory of Molecular Biology, National Cancer Institute, Bethesda, Maryland 20892, USA

ABSTRACT

The *Bacillus subtilis* genome is predicted to encode numerous ribonucleases, including four 3' exoribonucleases that have been characterized to some extent. A strain containing gene knockouts of all four known 3' exoribonucleases is viable, suggesting that one or more additional RNases remain to be discovered. A protein extract from the quadruple RNase mutant strain was fractionated and RNase activity was followed, resulting in the identification of an enzyme activity catalyzed by the YloC protein. YloC is an endoribonuclease and is a member of the highly conserved "YicC family" of proteins that is widespread in bacteria. YloC is a metal-dependent enzyme that catalyzes the cleavage of single-stranded RNA, preferentially at U residues, and exists in an oligomeric form, most likely a hexamer. As such, YloC shares some characteristics with the SARS-CoV Nsp15 endoribonuclease. While the *in vivo* function of YloC in *B. subtilis* is yet to be determined, YloC was found to act similarly to YicC in an *Escherichia coli* *in vivo* assay that assesses decay of the small RNA, RyhB. Thus, YloC may play a role in small RNA regulation.

Keywords: bacteria; *Bacillus*; endoribonuclease; oligomer; small RNA processing

INTRODUCTION

Messenger RNA turnover is an essential function of bacteria, allowing timely pivoting of gene expression programs to adapt to changing environmental conditions, as well as providing free ribonucleotides to the pool used for new transcription. In *Escherichia coli* and *Bacillus subtilis*, the organisms in which mRNA decay has been most widely studied, mRNA turnover is thought to initiate primarily with an endonucleolytic cleavage in the body of the message, followed by processive exonucleolytic degradation. Decay-initiating cleavages are catalyzed primarily by RNase E in *E. coli* and RNase Y in *B. subtilis* (Lehnik-Habrink et al. 2012; Mackie 2013). In *E. coli*, exonucleolytic decay of mRNA is mediated by two 3'-to-5' exoribonucleases: polynucleotide phosphorylase (PNPase) and RNase II. A strain that is missing both of these activities is inviable (Donovan and Kushner 1986). In *B. subtilis*, exonucleolytic decay can occur in the 5'-to-3' direction by RNase J1 (Condon 2010), and in the 3'-to-5' direction by one or more of the four 3' exonucleases known to exist in *B. subtilis*: PNPase, RNase R, RNase PH, and YhaM (Bechhofer and

Deutscher 2019). Previous biochemical (Wang and Bechhofer 1996) and RNA-seq (Liu et al. 2014) studies in *B. subtilis* suggested that PNPase is the major 3' exonuclease involved in mRNA decay. In a strain that is missing PNPase, decay intermediates accumulate (Bechhofer and Wang 1998; Oussenko et al. 2005), and a third of expressed genes show a significant increase in the ratio of 5'/3' RNA-seq reads (Liu et al. 2014). The other *B. subtilis* 3' exonucleases, or their orthologues, have known functions: RNase PH, tRNA processing (Wen et al. 2005); RNase R, rRNA quality control (Deutscher 2009); and YhaM, mRNA trimming at the 3' end (Broglia et al. 2020).

We previously constructed strains of *B. subtilis* that are missing one, two, or three of the known 3' exonucleases (Bechhofer et al. 2008). It appears that, in the absence of PNPase, other 3' exonucleases can compensate in the mRNA decay pathway. In fact, while the PNPase mutant strain has several interesting phenotypes (Wang and Bechhofer 1996), some of which have been linked to an inability to rapidly degrade the mRNA encoding the

© 2022 Ingle et al. This article is distributed exclusively by the RNA Society for the first 12 months after the full-issue publication date (see <http://majournal.cshlp.org/site/misc/terms.xhtml>). After 12 months, it is available under a Creative Commons License (Attribution-NonCommercial 4.0 International), as described at <http://creativecommons.org/licenses/by-nc/4.0/>.

Corresponding author: david.bechhofer@mssm.edu

Article is online at <http://www.majournal.org/cgi/doi/10.1261/ma.078962.121>.

regulatory protein, SlrA (Liu et al. 2016), this strain grows almost as well as wild type in laboratory conditions. Thus, it appears that mRNA decay can be accomplished by redundant activities. We also constructed a strain that was missing all four known 3' exonucleases: PNPase, RNase PH, RNase R, and YhaM (Oussenko et al. 2005). This "quadruple mutant" strain had a slow-growth phenotype, with a generation time measured at 101 min. The ability to obtain a viable strain without all known 3' exonucleases suggested that mRNA turnover could be accomplished in this strain either in the 5'-to-3' direction by the 5' exonuclease, RNase J1, or by an as yet unknown 3' exonuclease. In this study, we assayed RNase activity in a protein extract from the quadruple mutant strain, anticipating that we would find a fifth 3' exonuclease. We indeed discovered a new ribonuclease, encoded by the *yloC* gene. Contrary to expectations, YloC demonstrated *in vitro* endonuclease, rather than 3' exonuclease, activity. We report on the biochemical properties of this novel ribonuclease and suggest its function, based on the function of the homologous YicC protein of *E. coli*.

RESULTS

Identification of a new *B. subtilis* endoribonuclease

Bacillus subtilis strain BG505 is a derivative of the wild-type strain, BG1, that carries gene disruptions of the four known 3'-to-5' exoribonucleases (Supplemental Table S1), as reported previously (Oussenko et al. 2005). A protein extract of BG505 was prepared as described in Materials and Methods, and ribonuclease activity in the extracts was assayed using a 36-nt RNA substrate that was labeled at the 5' end with the LI-COR fluorophore IRDye 800 (DHB1879) (Supplemental Table S2). This substrate was designed to have minimal predicted secondary structure and to be of a size that large and small cleavage products containing the labeled end could be resolved on a 15% denaturing polyacrylamide gel. The results of a ribonuclease assay in cell extracts showed a limit product of ~5–7 nt, in the presence or absence of added inorganic phosphate, indicating a hydrolytic activity (Fig. 1A). Total protein from the BG505 extract was subjected to a series of fractionations (see Materials and Methods), and RNase activity was followed with the IR800-labeled RNA. After the final step of size-exclusion chromatography, the fraction with activity was separated on a 4%–12% Bis–Tris gel and two major bands were cut out from the gel and submitted for LC–MS–MS mass

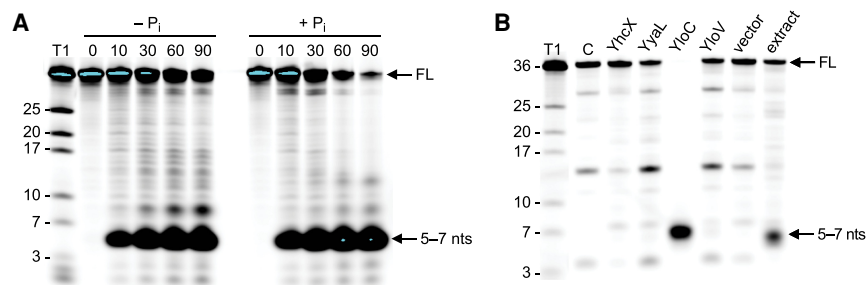


FIGURE 1. RNase activity *in vitro*. (A) Assay for RNase activity in a dialyzed protein extract from BG505, the quadruple 3' exonuclease mutant strain. [IR800]5'-end-labeled RNA oligonucleotide (oligo) incubated at 37°C for time (in minutes) indicated above each lane, with or without added inorganic phosphate. T1 lane is the same oligo digested with RNase T1, which cleaves after G residues. Numbers at the left indicate migration of T1 digestion products. Migration of full-length 36-nt RNA (FL) and limit digestion products of 5–7 nt indicated at the right. (B) Test of candidate proteins for RNase activity. IR800-labeled RNA oligo was incubated for 30 min at 37°C. (C) Control lane with no added protein. Purified 8×His-Sumo-tagged proteins indicated above each lane. (Vector lane) RNase digest with protein from a strain carrying the pET-57 vector without the insert. (Extract lane) RNase digest with protein extract from BG505.

spectrometry analysis and sequencing. Of 40 peptide matches to *B. subtilis* proteins, four candidate proteins were chosen that were of undetermined function and that could possibly specify enzymatic activity: YhcX, YloC, YloV, and YyaL. According to the Subtiwiki site (Zhu and Stulke 2018), YhcX belongs to the carbon–nitrogen hydrolase superfamily; YloC is a UPF0701 family member, similar to YicC of *E. coli*; and YloV, also called FakA, is a putative fatty acid kinase. There is no information on a possible function for YyaL. Disruptions of each of the genes encoding these proteins were obtained and none of the disrupted strains showed any overt phenotypes.

Coding sequences of these four genes were amplified by PCR and cloned in a modified pET57 vector that contained amino-terminal 8×His and Sumo tags (Lazarus et al. 2015). Expression of cloned coding sequences was induced in 10-mL cultures and His-tagged protein was purified by nickel column chromatography. Three of the tagged proteins (YyaL, YloC, and YloV) showed high yield and good purity (Supplemental Fig. S1). YhcX was poorly expressed but gave enough protein to assay for enzymatic activity. The ribonuclease assay (Fig. 1B) showed clearly that only YloC digested the RNA substrate to a limit product that was similar in size to that found in the BG505 extract (Fig. 1A). Thus, we identified YloC as a new *B. subtilis* ribonuclease.

To observe possible decay intermediates, the RNase assay was repeated with dilutions of input YloC protein. The results (Fig. 2A) indicated the presence of several decay intermediates at dilute enzyme conditions. A time course showed an accumulation of the 5- to 7-nt products over time, but no accumulation of the intermediate products (Fig. 2B). There were no cleavage products shorter than the 5-nt fragment (Supplemental Fig. S2).

Decay intermediates could be due to pausing of 3' exonuclease processivity or could be the result of

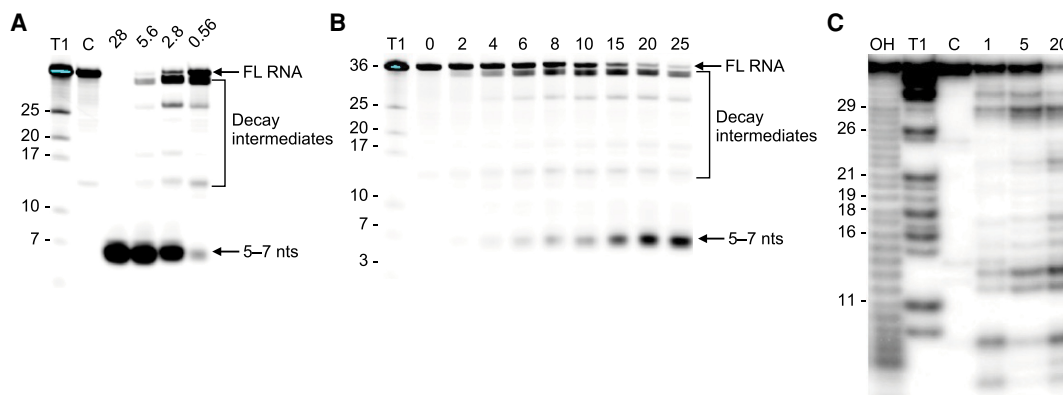


FIGURE 2. YloC is an endoribonuclease. (A) YloC activity with varied substrate:enzyme ratios. An amount of 30 pmol of RNA oligo (labeled + unlabeled) was incubated for 30 min at 37°C with decreasing concentrations (picomoles) of tagged YloC protein, as indicated above each lane. (T1) T1 RNase digest. Size of T1 digestion products indicated at the left. (C) Control lane with no protein added. (B) YloC activity at short time points. An amount of 30 pmol of RNA oligo (labeled + unlabeled) was incubated at 37°C with 10 pmol of tagged YloC protein and aliquots were removed at times (in minutes) indicated above each lane. (C) YloC activity on [³²P]3'-end-labeled RNA oligo. (OH) RNA oligo treated with hydroxyl, (T1) T1 RNase digest. Size of T1 cleavage products (nucleotides), ending with the nucleotide immediately succeeding the target G residue, indicated at the left.

endonuclease cleavage. To distinguish between these possibilities, the RNA substrate was labeled at the 3' end with [5'-³²P]cytidine 3',5' bis(phosphate)—pCp (Nilsen 2014). If YloC acted as a 3' exonuclease and degraded processively from a free 3' hydroxyl, the only product that would be observed on a gel would be the labeled single nucleotide. However, the data in Figure 2C show a number of cleavage intermediates, demonstrating clearly that YloC cleaves endonucleolytically. Thus, YloC is an endoribonuclease.

YloC protein sequence

The YloC coding sequence (291 amino acids; molecular weight 33.48 kDa) was not predictive of an RNase activity, suggesting that YloC represents a previously unknown type of ribonuclease enzyme. Based on the amino-terminal domain homology with *E. coli* YicC (Fig. 3A), YloC is listed in the UniProt UPF catalog (uncharacterized protein families) as a member of UPF0701, consisting of *E. coli* YicC, *B. subtilis* YloC, and *H. influenzae* Y467. In fact, YloC-like proteins are widespread in the bacteria, and an alignment of the YloC amino acid sequence with homologous proteins from diverse organisms shows clear sequence conservation in the amino-terminal region, and even more so in the carboxy-terminal domain (Fig. 3B). According to the Pfam categorization of domains that cannot be reliably annotated from the literature (Bateman et al. 2010), the carboxy-terminal domain of YloC (residues 207–291) is characterized as “DUF1732” or “domain of unknown function 1732.” Strikingly, in a compilation of 3472 bacterial DUFs, DUF1732 is ranked number 20 of the top 24 DUFs that are present in 500 or more species and are distributed over the great majority of bacterial phyla (Goodacre et al.

2013). There are no structures available in the protein structure data banks for any YloC homolog.

Biochemical properties of YloC

In order to examine YloC's biochemical properties, the 8×His-Sumo tag was detached by Sumo protease digestion, followed by nickel column chromatography to remove the tag. YloC RNase activity was dependent on the presence of a divalent cation (Fig. 4A), and our standard assay conditions included 2.5 mM Mg²⁺. YloC was active in the presence of Mg²⁺, Mn²⁺, and Co²⁺, but was not active in the presence of Ca²⁺, Cu²⁺, and Zn²⁺. As measured by the initial rate of accumulation of the 5- to 7-nt product, YloC was actually more active in the presence of Mn²⁺ than in the presence of Mg²⁺ (Fig. 4B).

To determine the nature of the 3' end left after cleavage, we tested whether the YloC cleavage products could be ligated by T4 RNA ligase to a DNA oligonucleotide (oligo) to which an adenylate ribonucleotide was added at the 5' end. The DNA oligo carried a cytidylate dideoxynucleotide at the 3' end to block self-ligation. If YloC cleavage generated a 3' phosphate and a 5' hydroxyl, ligation to the DNA oligo would depend on prior removal of the 3' phosphate group by the 3'-phosphatase reaction of T4 polynucleotide kinase (Cameron and Uhlenbeck 1977). If YloC cleavage generated a 3' hydroxyl and a 5' phosphate, ligation would occur without such treatment. As can be seen in Figure 4C, not only the full-length RNA substrate, which has a 3' hydroxyl end, could be ligated to the DNA oligo, but YloC cleavage products could also be ligated to the DNA oligo, even without prior polynucleotide kinase treatment. Thus, YloC cleaves to leave a 3' hydroxyl and, presumably, a 5' phosphate.

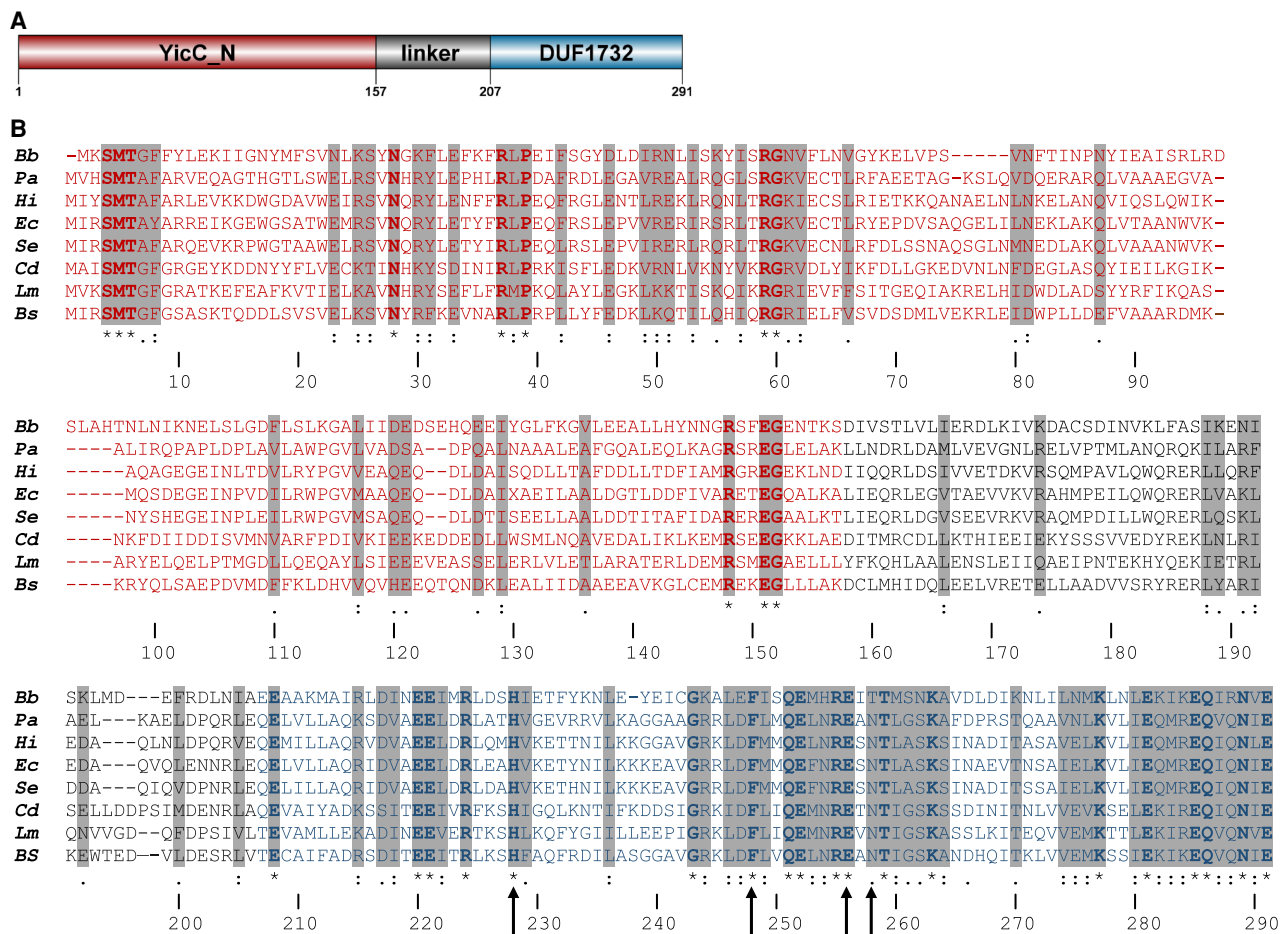


FIGURE 3. YloC domain structure and primary sequence. (A) Domain structure of YloC, as predicted by the Pfam database of protein families (Mistry et al. 2021). (B) CLUSTAL alignment of YloC-like proteins from eight organisms. Amino acid residues in domains are colored as in the schematic in part A. Two-letter abbreviations: (Bb) *Borrelia burgdorferi*, (Pa) *Pseudomonas aeruginosa*, (Hi) *Haemophilus influenzae*, (Ec) *Escherichia coli*, (Se) *Salmonella enterica*, (Cd) *Clostridia difficile*, (Lm) *Listeria monocytogenes*, (Bs) *Bacillus subtilis*. Upward-pointing arrows below the alignment point to residues (H228, F248, E256, and N258) that were mutated to alanine. Asterisks indicate identical residues in all species. Two dots indicate conserved residues. One dot indicates similar residues. Regions of high homology are shaded.

YloC cleavage specificity

To explore possible cleavage specificity of YloC, ribonuclease activity was assayed on 5'-³²P-end-labeled RNA oligos. While the IR800-labeled RNA substrate was suitable for initial characterization of YloC cleavage activity, we chose to use substrates with a native 5' phosphate to determine target sequence specificity, if any. In designing oligos for this purpose, we were interested in following up on the observation (seen clearly in Supplemental Fig. S2) that major cleavages appeared at nucleotides 5–7, which is an AUG sequence (Supplemental Table S2, DHB1866 sequence). This raised the possibility that YloC has specificity for a start codon sequence. As such, 26-nt oligos were designed with either the same sequence as the first 26 nt of DHB1866 (DHB1935), or with an AUG sequence located at nucleotides 13–15 (DHB1922). These oligos were designed to avoid having any predicted secondary

structure. The YloC cleavage pattern for these two oligos (Fig. 5A) did not show a particular specificity for the AUG sequence. Two other oligos were used with an AUG sequence at nucleotides 10–12 (DHB1921 and DHB1923) with different surrounding sequences (Supplemental Fig. S3). From the patterns of YloC digestion for these four oligos, we could not discern any specific cleavage target(s).

[³²P]5'-end-labeled oligonucleotides consisting of a single base type were used to determine whether YloC has a preference for specific nucleotides. The results (Fig. 5B) indicated a preference for pyrimidines, with poly(U) nucleotide being preferred over poly(C). The poly(A) oligo showed barely any cleavage, and the poly(G) oligo showed weak cleavage at a few sites, which was possibly an effect of structure conferred by G base repeats (Burge et al. 2006). So far, we have not determined whether YloC cleaves 5' or 3' of pyrimidine residues.

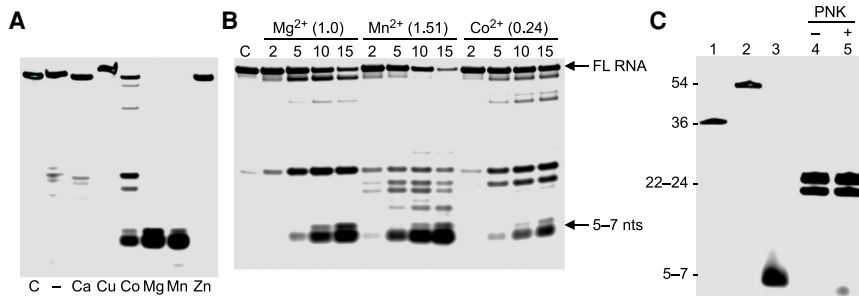


FIGURE 4. Biochemical characterization of YloC ribonuclease activity. (A) Metal-ion dependence of YloC activity. An amount of 30 pmol of RNA oligo (IR800-labeled + unlabeled) was incubated with 10 pmol of YloC for 20 min at 37°C. Abbreviations of divalent cations: (Ca) Calcium, (Cu) copper, (Co) cobalt, (Mg) magnesium, (Mn) manganese, (Zn) zinc. All reactions were with 2.5-mM divalent cation. (C) Control lane with no protein. (B) Initial rate of YloC cleavage, as measured by appearance of 5- to 7-nt product, in the presence of indicated divalent metal cation (2.5 mM) at 37°C. Numbers in parentheses are the initial rate of product formation, relative to the initial rate in the presence of Mg^{2+} (average of two experiments). (C) Determination of the nature of the 3' end after YloC cleavage. (Lane 1) IR800-labeled 36-nt RNA oligo. (Lane 2) Thirty-six-nucleotide RNA ligated to 18-nt DNA oligo. (Lane 3) Five-nucleotide to 7-nt products from 36-nt RNA oligo after incubation with YloC for 20 min at 37°C. (Lanes 4,5) Ligation of 5- to 7-nt YloC cleavage products to 18-nt DNA oligo without or with prior polynucleotide kinase (PNK) treatment, as indicated. Sizes of RNA and RNA–DNA products (nucleotides) are indicated at the left.

We tested whether YloC can act on double-stranded RNA. 5'-End-labeled DHB1935 was incubated in the presence of an excess of either unlabeled sense RNA (i.e., the same sequence as DHB1935) or unlabeled antisense RNA (i.e., complementary to DHB1935). The results in Figure 5C show that YloC has minimal activity on double-stranded RNA. In addition, we tested whether YloC has activity on DNA, using a DNA oligo that had the same sequence as DHB1935. No cleavage was observed (Fig. 5C).

Ribonuclease activity of YloC mutant proteins

Rudimentary models for YloC structure were constructed using HHpred (Soding et al. 2005) and Phyre2 (Kelley et al. 2015) software, which suggested residues in the highly conserved carboxy-terminal domain that might be involved in catalysis. The conserved H228 and E256 residues were mutated to alanines and cleavage activity on the IR800-labeled substrate was assessed. YloC H228A and E256A showed drastically reduced activity (Fig. 6), giving 0.26% and 0.22% of wild-type activity, respectively, as measured by the initial rate of formation of the 5- to 7-nt products. This result suggested that the carboxy-terminal domain may contain the enzyme active site. On the other hand, an N258A YloC protein gave 11.1% activity, suggesting that highly conserved residues in the carboxy-terminal domain may not be absolutely required for ribonuclease function. An F248A YloC protein, as well as a YloC protein that was missing the first 10 residues, did not express well in *E. coli*, and were not tested for activity. Notably, the effect of mutations on YloC activity demon-

strated that the ribonuclease activity being measured in our assays was due to YloC itself, and was not the result of contaminating RNase activity from *E. coli*.

E. coli YicC ribonuclease activity

The *E. coli* *yicC* gene encodes a non-essential protein that is 30% identical and 52% similar to YloC. We tested YicC for ribonuclease activity and found that the cleavage pattern for the IR800-labeled substrate was identical to that of YloC, with a somewhat slower initial rate of cleavage (Fig. 7). Similarly, YicC protein gave the same pattern as YloC for [^{32}P]5'-end-labeled substrates (Fig. 5A).

YloC in vivo function

As mentioned above, a *B. subtilis* strain that was deleted for the *yloC* gene showed no overt growth phenotype. Since YloC has RNase activity, we assessed whether the *yloC* knock-out could coexist with deletions of other ribonuclease genes. Combining *yloC* and *pnpA* (encoding PNPase) gene deletions did not result in an observable growth phenotype (Supplemental Fig. S4). We constructed several mutant strains that were deleted for *yloC* and three, or even four, ribonuclease-encoding genes (Supplemental Table S1). We did not observe additional phenotypes that were due to the absence of YloC.

While these experiments were in progress, Chen et al. (2021) reported that *E. coli* YicC is involved in regulating the level of the iron-responsive small RNA (sRNA), RyhB. RyhB inhibits translation of *sodB* mRNA, encoding superoxide dismutase, by binding to the *sodB* mRNA ribosome binding site and start codon. A fluorescence assay, using a chromosomal *sodB*-mCherry translation fusion, was devised to monitor RyhB repression of *sodB* expression in the presence of shotgun-cloned genes from *E. coli* (Fig. 8A). Chen et al. (2021) found that expression of YicC from a medium- or high-copy plasmid led to rapid decay of RyhB and thus increased fluorescence from the *sodB*-mCherry reporter fusion. The rapid decay of RyhB also required PNPase activity (see Discussion). The in-cell reporter system provides an excellent tool to measure YicC activity in vivo. To assess whether YloC has a similar in vivo function, the *yloC* gene was cloned into the medium-copy number pQE80L plasmid that was used for the *E. coli* fluorescence assay. Expression of YloC in the *E. coli* reporter strain resulted in increased fluorescence, as measured by a microplate reader and fluorescence

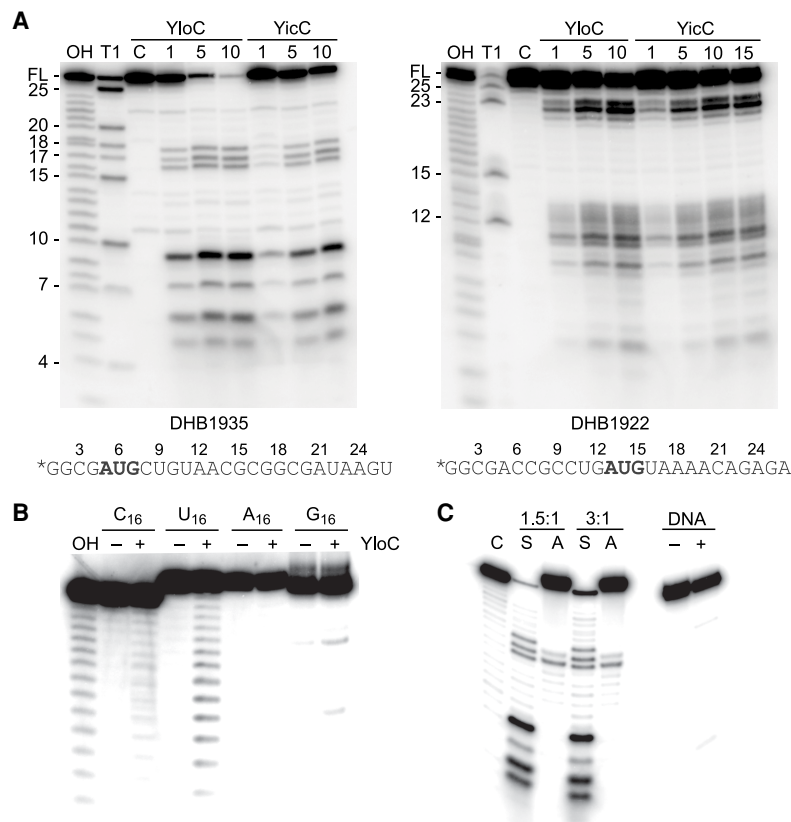


FIGURE 5. Nucleotide target specificity of YloC. (A) YloC (and YicC) cleavage pattern on [³²P] 5'-end-labeled RNA oligos with different 26-nt sequences. The AUG sequence of each oligo is in bold. An amount of 30 pmol of RNA (labeled + unlabeled) was incubated with 10 pmol of YloC at 25°C for the indicated times (in minutes). (OH) RNA oligo treated with hydroxyl, (T1) T1 RNase digest. Migration of full-length (FL) RNA and T1 RNase digestion products indicated at the left. (B) YloC activity on polynucleotides containing a single base type indicated above each set of lanes. (C) Assay of YloC activity on [³²P]-labeled DHB1935 in the presence of an excess (1.5-fold or threefold) of unlabeled sense (S) or antisense (A) RNA. Lanes at right contained a [³²P]5'-end-labeled DNA oligo, with the same sequence as DHB1935, in the absence (-) and presence (+) of YloC.

microscopy, similar to what was observed with the cloned *yicC* gene (Fig. 8B,C).

Further experiments were performed with the *E. coli* strain expressing YloC to demonstrate that YloC functions similarly to YicC. First, the level of RyhB RNA was analyzed by northern blot on total RNA isolated from strains expressing YicC, YloC, and a control strain expressing neither protein. The results (Fig. 8D,E) show that there was a significant decrease (approximately threefold) in the level of RyhB in a strain expressing YloC. The decrease in RyhB was not as large as for the strain expressing YicC, as could be expected from the difference in the fluorescence fold change between these two strains (Fig. 8C). Next, we tested whether there is an *in vivo* interaction between YloC and PNPase in *E. coli*, using the bacterial two-hybrid assay (Karimova et al. 2000). Plasmid-borne versions of the YicC or YloC coding sequence and the PNPase coding sequence were fused to the adenylate cyclase amino-termi-

nal T25 or carboxy-terminal T18 domain (see Materials and Methods). The results of the β-galactosidase assay are shown in Figure 8F, and the colony assay is shown in Supplemental Figure S6. These results demonstrated a strong interaction between YloC and PNPase.

YloC potentially exists as a hexamer

In preliminary experiments to establish conditions for YloC crystallization, a large amount of purified YloC was isolated from *E. coli* (see Materials and Methods). After cleavage of the 8×His-Sumo tag, YloC protein was fractionated on an FPLC column. The result in Figure 9 showed that the 33.5-kDa YloC exists in solution predominantly in an oligomeric form, with a molecular weight of >160 kDa. A study of oligomeric forms of proteins in various species, including *B. subtilis*, showed that pentameric forms are rare and heptameric forms are highly unlikely, whereas hexamers are more prevalent (Danielli et al. 2020). Thus, we tentatively conclude that YloC exists as a hexamer.

DISCUSSION

We have discovered an enzyme with endoribonucleolytic activity, encoded

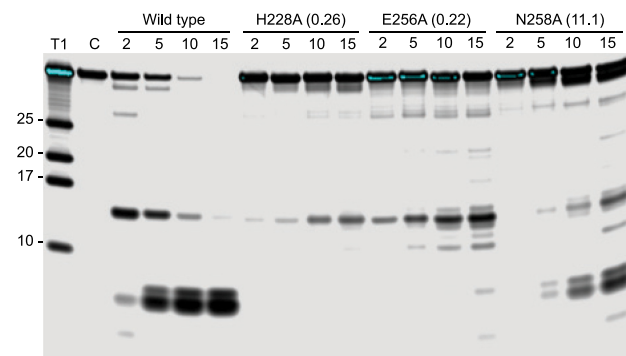


FIGURE 6. RNase activity of YloC mutant proteins. An amount of 30 pmol RNA oligo (IR800-labeled + unlabeled) was incubated at 37°C with 10 pmol of wild-type or mutant YloC protein for the times (in minutes) indicated above each lane. Numbers in parentheses are the initial rate of product formation, relative to the initial rate for the wild type (average of three experiments).

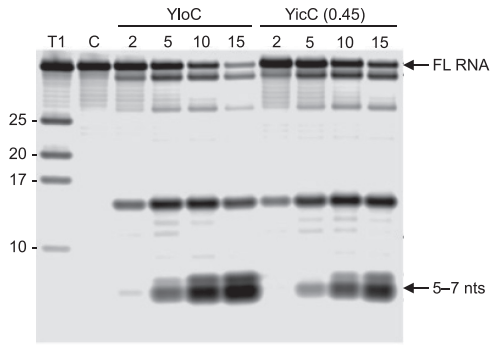


FIGURE 7. YicC and YloC have similar activities. RNase activity of *E. coli* YicC protein compared with *B. subtilis* YloC protein, on IR800-labeled RNA oligo. An amount of 30 pmol of RNA (labeled + unlabeled) was incubated at 37°C with 10 pmol of YicC or YloC protein for the times (in minutes) indicated above each lane. The number in parentheses is initial rate of product formation, relative to the initial rate for YloC (average of two experiments).

by the *B. subtilis* *yloC* gene, which appears to represent a new RNase family. *yloC* homologs are widespread in bacteria, and the alignment in Figure 3 shows the high degree of conservation among diverse pathogenic species, especially in the amino-terminal and carboxy-terminal regions. Modeling of the carboxy-terminal domain, known as DUF1732, suggested that this was a nucleic acid-binding domain (Rigden 2011). Our finding that mutants of conserved histidine and glutamate residues in the carboxy-terminal domain almost completely abolished RNase activity

(Fig. 6) suggests that these residues may be part of the active site or may interact with the divalent cation that is required for the activity (Fig. 4A).

The fact that YloC cleaves to leave a 3' hydroxyl (Fig. 4C) is expected for a metal-ion-dependent endonuclease (Saida et al. 2003). Interestingly, although Mg^{2+} , Mn^{2+} , and Co^{2+} could support YloC activity, the preferred metal ion was Mn^{2+} (Fig. 4B). This characteristic is reminiscent of the NendoU family RNase of SARS-CoV endonuclease, Nsp15, which is active in the presence of Mg^{2+} but is much more active in the presence of Mn^{2+} (Bhardwaj et al. 2004). However, Nsp15 generates a 2'-3' cyclic phosphate end (Ivanov et al. 2004; Bhardwaj et al. 2006), which is characteristic of metal-independent RNases, like RNase A. It has been proposed that the Nsp15 catalytic mechanism, in fact, does not involve metal ions and the effect of Mn^{2+} is to increase binding affinity for the RNA substrate (Bhardwaj et al. 2006). Experiments are in progress to examine the RNA-binding properties of YloC.

Using [^{32}P]5'-end-labeled RNA oligos, we could not determine features of the RNA that could confer higher affinity for the substrate (Fig. 5A; Supplemental Fig. S3). The analysis of cleavage fragments was complicated by the potential for multiple cleavages occurring on the same molecule. As such, band intensities could not be used to assess the preference of target nucleotides, since the intensity of a band that represents cleavage at a 3'-proximal site was likely to be reduced by intervening cleavages between the downstream cleavage site and the 5' end. On the other

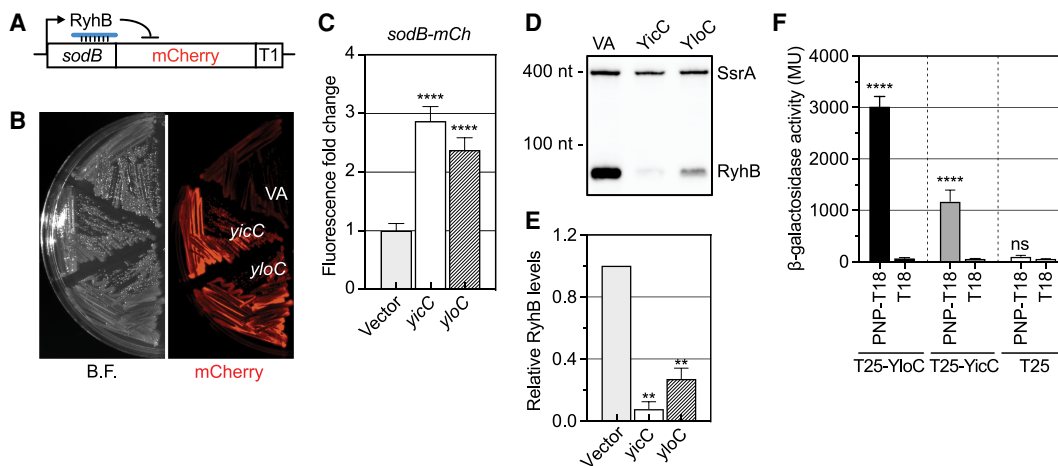


FIGURE 8. Heterologous expression of *B. subtilis* *yloC* in *E. coli* disrupts RyhB sRNA regulation. (A) Schematic of the *sodB* translational reporter fusion for monitoring RyhB sRNA activity in *E. coli* (Chen et al. 2021). (B) Imaging colony fluorescence on an agar plate. (VA) Vector alone, (B.F.) bright field, (mCherry) fluorescence. (C) Quantitation of mCherry fluorescence; an average of four biological repeats. (****) $P < 0.0001$. (D) The same set of strains was subjected to northern blot analysis of RNA, with probing for RyhB RNA and the control SsrA RNA, as well as total protein extraction and Coomassie staining (Supplemental Fig. S5). (E) Relative levels of full-length RyhB were quantitated from two independent experiments, normalized to the SsrA loading control first, and then further compared with that of the vector control. Unpaired two-tailed Student's *t*-test was used to calculate statistical significance. (**) $P < 0.01$. (F) Bacterial two-hybrid test for YloC interaction with PNPase. The reporter strain BTH101 was cotransformed with plasmids T18 and T25 fused to PNPase, YicC, or YloC and assayed for β -galactosidase activity. Data are the mean and standard deviation of biological triplicates. Two-way ANOVA was used to calculate statistical significance. (ns) Not significant, $P > 0.05$; (****) $P < 0.0001$.

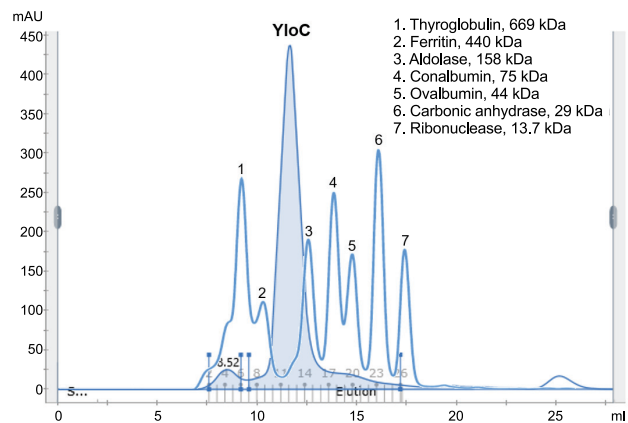


FIGURE 9. FPLC elution profile of YloC, superimposed on elution profiles of molecular weight standards. Control peaks are numbered with the respective molecular weights (in kilodaltons) indicated.

hand, the experiment with polynucleotides containing a single base indicated that YloC has a preference for pyrimidines, but especially poly(U) (Fig. 5B). Poly(C) was also cleaved, but not as much. Higher activity with the poly(U) substrate is similar to the preferences reported for the SARS-CoV Nsp15 RNase (Bhardwaj et al. 2006) and the related XendoU endoribonuclease from *Xenopus laevis* (Laneve et al. 2003). The specificity of YloC for single-stranded RNA, rather than double-stranded RNA (Fig. 5C), is also consistent with the preference of Nsp15 for unpaired U residues (Bhardwaj et al. 2006). Recently, the ability of Nsp15 to cleave the poly(U) tail of negative-strand viral RNA was shown to be important for the evasion of host defenses (Hackbart et al. 2020).

By FPLC chromatography, it appears that the dominant form of YloC is an oligomer of >160 kDa (Fig. 9), most likely a hexamer. This is yet another way in which YloC is similar to SARS-CoV Nsp15, which exists and functions as a hexamer (Guarino et al. 2005; Ricagno et al. 2006; Bhardwaj et al. 2008). One other bacterial RNase, the 3' exonuclease RNase PH, also exists and functions as a hexamer (Ishii et al. 2003; Choi et al. 2004); however, RNase PH is a phosphorolytic enzyme. Interestingly, *E. coli* YicC also exists in an oligomeric form (Chen et al. 2021). Efforts are underway to crystallize YloC, so that the residues involved in catalysis and multimer formation can be identified. It should be noted that there is relatively little overall sequence homology between YloC and Nsp15. A local alignment (Madeira et al. 2019) could identify regions in the two proteins (YloC residues 54–146 and Nsp15 residues 240–334) that showed 21% identity and 55% similarity.

We do not know the function of YloC in *B. subtilis*. A *yloC* knockout strain, as well as several ribonuclease gene knockout strains that included the *yloC* disruption, did not show any phenotypes related to *yloC* when grown in rich liquid media or on solid media. A very recent publication reported that the CD25890 protein of *C. difficile*,

which shares 40% identity and 63% similarity to YloC, is involved in sporulation initiation (Martins et al. 2021). We tested the *yloC* knockout strain for any sporulation defect and found no effect (DH Bechhofer, unpubl.). However, we did find an effect of YloC expression in *E. coli* on the regulatory RNA, RyhB, which was similar to the effect of native *E. coli* YicC expression (Fig. 8B–E). The experiments of Chen et al. (2021) suggested that RyhB RNA half-life is decreased when YicC protein is expressed from a plasmid. This effect was found to be dependent on the presence of the 3' exonuclease PNPase, and the model that was proposed for YicC function was that the protein acts as an adaptor that recruits PNPase to RyhB RNA, targeting it for degradation (Chen et al. 2021). Indeed, like YicC, YloC interacts with PNPase in vivo (Fig. 8F; Supplemental Fig. S6). On the other hand, we have shown that YicC has the same in vitro endoribonuclease activity as YloC (Figs. 5A, 7), which may suggest a different model in which YicC cleaves RyhB near the 3' end, allowing PNPase access for rapid degradation. The fact that cleavage products of RyhB were not observed when YicC was expressed could be explained by the rapid turnover of such cleavage products by PNPase or, in its absence, RNase II. In any event, based on the idea that the homologous YicC is an RNA-binding protein that functions as an adaptor in vivo, as well as the likely hexameric nature of YloC, it is tempting to speculate that YloC functions in a manner similar to the RNA-binding protein, Hfq, also a hexameric protein. While in *E. coli* Hfq plays a major role in facilitating small RNA regulation (Hor et al. 2020), the homologous protein in *B. subtilis* does not seem to have this sort of role, as evidenced by the lack of phenotype of a *B. subtilis* *hfq* deletion mutant in ~2000 different growth conditions (Rochat et al. 2015). Although we observe YloC endonuclease activity in vitro, it may function in vivo also as an RNA-binding protein that acts in post-transcriptional regulation. Much more needs to be learned about this highly conserved protein.

MATERIALS AND METHODS

Protein purification from the quadruple mutant strain

Bacillus subtilis strain BG505 (the quadruple 3' exoribonuclease mutant strain) was grown overnight at 37°C with vigorous shaking in Luria-Bertani (LB) medium in the presence of 100 µg/mL spectinomycin, and the cells were collected by centrifugation (5–8g). The cell pellet was washed with 200 mM KCl and resuspended in 40 mL of buffer A (20 mM Tris at pH 8.0, 60 mM KCl, 1 mM DTT, 0.2 mM PMSF, 0.1 mM EDTA, 5% glycerol). After treatment with 0.2 mg/mL lysozyme for 15 min at 37°C, the cells were disrupted in a French press. Streptomycin sulfate was added to 2% with stirring at 4°C, and the precipitate was removed by centrifugation at 20,000g for 15 min. Ammonium sulfate was added to

40% with stirring at 4°C. The precipitate was removed by centrifugation at 6000g for 15 min at 4°C, and the supernatant was dialyzed against buffer A. The supernatant contained 250–300 mg of total protein. Total protein was loaded onto DEAE Sepharose (GE Healthcare) in a 1.5-cm × 20-cm column that was equilibrated with buffer A. The column was washed copiously with buffer A, and then with buffer A containing 200 mM KCl. No RNase activity was lost in this step. The column was washed with buffer A containing 400 mM KCl and 15 fractions of 5 mL each were collected. Enzyme activity eluted in fractions 4–6, containing a total of 25–30 mg of protein (10-fold purification). Peak fractions were pooled, dialyzed against buffer A, and loaded onto Q Sepharose (GE Healthcare) in a 1.5-cm × 20-cm column that was equilibrated with buffer A. The column was washed extensively with buffer A and then with buffer A containing 200 mM KCl. Protein was eluted stepwise with buffer A containing 400 mM KCl and then 500 mM KCl, and 10 fractions of 2 mL each were collected from both elutions. Peak activity was eluted in the 500 mM KCl fractions 5–7, with a total protein content of 5–6 mg (50-fold purification). The peak activity fraction was dialyzed against buffer A and concentrated with a 0.5-mL Amicon Ultra filter unit (Millipore) to 200–300 µL for further purification by size-exclusion chromatography. Sephacryl S-200 (GE Healthcare) was loaded to a height of 20 cm in a 1-cm × 25-cm column. Protein (300 µL) was loaded on the column and washed with buffer A, and 300-µL fractions were collected. Peak activity was observed in fractions 24–30. Two major bands were cut out from a NuPAGE 4%–12% Bis–Tris gel (Invitrogen) and sent for LC–MS–MS mass spectrometry analysis and sequencing at the Stony Brook University School of Medicine spectrometry facility. High-confidence peptides were mapped to the *B. subtilis* proteome, using the Swiss-Prot database.

Cloning and expression

The *yhcX*, *yyaL*, *yloC*, and *yloV* coding sequences were amplified from wild-type *B. subtilis* genomic DNA and cloned into a modified pET-47b vector that had an amino-terminal Sumo fusion tag instead of the HRV3C cleavage site (Lazarus et al. 2015). Plasmids, including a control vector plasmid without insert, were transformed into *E. coli* Lemo21 (DE3) competent cells (New England Biolabs), and protein was isolated using Ni-NTA column purification (Qiagen) and eluted with 250 mM imidazole. Imidazole was removed by dialysis in buffer A. Proteins were analyzed for purity on a NuPAGE 4%–12% Bis–Tris gel. For initial screening of the candidate proteins, the RNase assay was carried out directly with tagged protein. For further biochemical experiments, tagged YloC was dialyzed in Tris buffer (Tris 20 mM, NaCl 100 mM, glycerol 10%) and incubated overnight with rotation at 4°C in the presence of a 250:1 ratio of protein:Sumo protease. The 8×His-Sumo tag was removed by Ni-NTA chromatography. Purified, untagged YloC protein was concentrated and exchanged with buffer A in a 0.5-mL Amicon Ultra filter unit. The *E. coli* *yicC* coding sequence was amplified from *E. coli* genomic DNA (DH5α) and cloned into the modified pET-47b vector. 8×His-Sumo-tagged YicC protein was treated with Sumo protease and purified as above for YloC. Site-directed mutagenesis of *yloC* and *yicC* codons was performed using the Quikchange II protocol (Agilent Technologies). Coding sequences containing mutations were confirmed by Sanger sequencing (Psomagen).

Ribonuclease assay

To follow RNase activity in protein extracts and to characterize YloC enzymatic activity, an RNA oligonucleotide (DHB1879) (Supplemental Table S2) was used that was labeled at the 5′ end with the LiCor IR800 dye (Integrated DNA Technologies). The standard RNase reaction contained 10 pmol of IR800-labeled RNA, 20 pmol of unlabeled RNA, and 20 µg of BSA, in a 45-µL volume of RNA assay buffer (5 mM MgCl₂, 50 mM Tris at pH 8.0, 7 mM NaCl, 100 mM KCl). The reaction was initiated by the addition of 5 µL (10 pmol) of either protein extract or purified YloC. At time points, 5 µL of the reaction mixture was removed and quenched with 5 µL of Ambion Gel Loading Buffer II and resolved on a 15% denaturing polyacrylamide gel. The gel was imaged directly on an Odyssey LiCor Imaging System.

For assays of YloC cleavage specificity, RNA oligonucleotides were labeled at either the 5′ end, with γ -³²P-ATP (PerkinElmer) and T4 polynucleotide kinase (New England Biolabs), or the 3′ end, with 5′-³²P-PcP (PerkinElmer), using the end-healing reaction (Nilsen 2014). After 3′-end labeling, the 3′-terminal phosphate was removed by phosphatase. Unincorporated ³²P-labeled nucleotide was removed by passage through a G50 spin column (GE Healthcare), and the labeled RNA was gel-purified on a 15% denaturing polyacrylamide gel. In a typical labeling reaction, 250 pmol of input RNA yielded 70–75 pmol of total RNA (labeled + unlabeled) after gel extraction. Approximately 200,000 cpm radioactivity was used in a 50-µL reaction. Cleavage products were resolved on a 0.4-mm-thick 18% denaturing polyacrylamide gel. The gel was run at 800 V (constant voltage). Upon completion of the run, the gel was fixed with 20% ethanol/10% acetic acid/3% glycerol solution for 15 min, transferred to a Whatman filter paper, and dried in a gel dryer. The gel was exposed to a GE Storage Phosphor Screen and imaged on a Typhoon Trio Imaging System (GE Healthcare). The gel image was processed with ImageJ software.

For the RNase T1 control ladder, labeled RNA (40,000 cpm) was treated with Ambion RNase T1, in accordance with the manufacturer's protocol. For the single-nucleotide control ladder, labeled RNA (40,000 cpm) was mixed with an equal volume of 1× alkaline hydrolysis buffer and 3 µg of yeast tRNA (Ambion). The reaction was incubated for 3 min at 95°C, placed for 2 min on ice, and mixed with an equal volume of Ambion Gel Loading Buffer II.

To analyze the base specificity of YloC, poly(A, U, C, and G) oligonucleotides (16 residues) were 5′-end-labeled and gel-purified, as described above. Approximately 20 pmol of labeled RNA was incubated with 5 pmol YloC at 37°C for 30 min in a 25-µL reaction. The reaction (2.5 µL) was mixed with 2.5 µL of Gel Loading Buffer II, resolved on an 18% denaturing polyacrylamide gel, and imaged as described above.

To assay for double-stranded RNA cleavage, 17 pmol of 5′-end-labeled DHB1935 was mixed with either unlabeled sense RNA (DHB1935) or antisense RNA (DHB1955) in a 1.5-fold or threefold molar excess of unlabeled to labeled RNA. Complementary RNA strands were annealed by being heated for 5 min to 95°C and then allowed to cool slowly to room temperature. RNA was treated with YloC for 30 min at 37°C and mixed with an equal volume of Gel Loading Buffer II. Prior to loading on an 18% denaturing gel, RNA was heated for 10 min to 95°C and then directly loaded onto the gel that was prerun at 25 W (constant wattage) to heat the gel to >60°C. The gel temperature was maintained at

>60°C, which was needed to maintain the labeled RNA in a single-stranded form.

3'-End identification

An amount of 30 pmol of RNA oligo (IR800-labeled + unlabeled) was treated with 10 pmol of YloC in a 30- μ L reaction for 1 h at 37°C in order to achieve complete digestion to the 5- to 7-nt limit product. Half of the reaction mixture was treated with T4 polynucleotide kinase (phosphatase plus; New England Biolabs) in a 20- μ L reaction for 30 min at 37°C. For the ligation reaction, 100 pmol of DNA oligo DHB1880 and T4 RNA Ligase (New England Biolabs) was added to both halves of the reaction mixture in the presence of 10% PEG800, and the mixture was incubated for 2 h at 25°C. As a control, 20 pmol of DHB1879 was ligated with the DNA oligo in a separate reaction. Reaction products were resolved on a 15% denaturing polyacrylamide gel.

sodB expression analysis

For agar plate measurement of *sodB* expression, the *sodB* reporter strain (JC1322) expressing *E. coli yicC* or *B. subtilis yloC* from the expression plasmid pQE80L (Qiagen), or vector alone, was grown on LB + ampicillin agar for 20 h at 37°C and imaged using the Bio-Rad ChemiDoc MP imager for bright field and for mCherry fluorescence. For liquid measurement, bacterial cultures on agar plates were resuspended in saline, and OD₆₀₀ as well as mCherry signals were measured using the BioTek microplate reader. Four biological repeats were measured for each strain, and data were plotted as mean and standard deviation. Unpaired two-tailed Student's *t*-test was used to calculate statistical significance.

Northern blot analysis

For northern blot analysis of *RyhB* RNA, 5 μ g of total RNA from each strain was resolved on a Bio-Rad Criterion 10% Tris-borate-EDTA (TBE)-urea polyacrylamide gel in 1 \times TBE buffer at 100 V for 1 h. The resolved RNA samples were then transferred to a Zeta-probe GT membrane (Bio-Rad) by wet electroblotting at 200 mA for 2 h in 0.5 \times TBE and cross-linked to the membrane by UV irradiation. The resulting membrane was hybridized with the biotinylated *ryhB* and *ssrA* probes in ULTRAhyb solution (Ambion) overnight at 42°C and further incubated with a streptavidin-conjugated alkaline phosphatase. The blot was then developed using the BrightStar BioDetect kit (Ambion) according to the manufacturer's instructions. Northern blots were imaged by capturing the chemifluorescence using the Bio-Rad ChemiDoc MP imager.

Large-scale purification of YloC

The strain with cloned wild-type YloC (EG1103) was grown overnight at 37°C in LB + kanamycin (50 μ g/mL) and was diluted 1:100 in 3 L of LB medium containing 1 mM MgSO₄ and kanamycin (40 μ g/mL). Cells were grown at 37°C to OD₆₀₀ of 0.6, at which point *yloC* expression was induced by the addition of 400 μ M IPTG for 3 h. Cells from each of the three 1-L volumes were collected by centrifugation at 5000g for 10 min at 4°C. (Following is for one pellet.) The cell pellet was resuspended in 35 mL of

cold 1 \times Tris-buffered saline (TBS; 20 mM Tris at pH 8.0, 250 mM NaCl) and centrifuged at 5000g for 10 min at 4°C. The pellet was stored at -80°C. The pellet was resuspended in 80 mL of 1 \times TBS and split into two aliquots. To each aliquot was added lysozyme to 100 μ g/mL, PMSF to 1 mM, and DNase (Roche) to 25 ng/mL, with incubation for 20–30 min on ice. The cell suspension was passed through a French press three times and the lysate was cleared by centrifugation at 8000g for 10 min at 4°C. The supernatant was centrifuged at 96,000g for 20 min at 4°C, and tagged YloC protein was purified with Ni-NTA column chromatography. Protein was eluted with 250 mM imidazole and concentrated on an Amicon ultra-15 concentrator (10-kDa cutoff) to 14 mL. The yield from 3 L of culture was ~24 mg of tagged YloC protein. Total protein was incubated overnight in a dialysis cassette at 4°C in the presence of a 250:1 ratio of protein:Sumo protease. The dialysis buffer was buffer A without EDTA. YloC was reverse-purified by Ni-NTA chromatography, and the final yield of YloC protein was ~13 mg. YloC protein was concentrated in an Amicon ultra-15 concentrator, and the final 1-mL volume was centrifuged twice at 21,000g for 5 min at 4°C to remove the precipitate. YloC protein was further purified by size-exclusion chromatography on a Superdex 200 increase column (GE AKTA pure instrument) in 1 \times TBS.

SUPPLEMENTAL MATERIAL

Supplemental material is available for this article.

ACKNOWLEDGMENTS

We thank Ciarán Condon for the initial modelling of YloC that suggested amino acid residues to be targeted for mutagenesis. Support was provided by the National Institutes of Health (GM-125655) to D.H.B. This research was also supported in part by the Intramural Research Program of the National Institutes of Health Center for Cancer Research.

Received August 24, 2021; accepted November 2, 2021.

REFERENCES

- Bateman A, Coggill P, Finn RD. 2010. DUFs: families in search of function. *Acta Crystallogr Sect F Struct Biol Cryst Commun* **66**: 1148–1152. doi:10.1107/S1744309110001685
- Bechhofer DH, Deutscher MP. 2019. Bacterial ribonucleases and their roles in RNA metabolism. *Crit Rev Biochem Mol Biol* **54**: 242–300. doi:10.1080/10409238.2019.1651816
- Bechhofer DH, Wang W. 1998. Decay of *ermC* mRNA in a polynucleotide phosphorylase mutant of *Bacillus subtilis*. *J Bacteriol* **180**: 5968–5977. doi:10.1128/JB.180.22.5968-5977.1998
- Bechhofer DH, Oussenko IA, Deikus G, Yao S, Mathy N, Condon C. 2008. Analysis of mRNA decay in *Bacillus subtilis*. *Methods Enzymol* **447**: 259–276. doi:10.1016/S0076-6879(08)02214-3
- Bhardwaj K, Guarino L, Kao CC. 2004. The severe acute respiratory syndrome coronavirus Nsp15 protein is an endoribonuclease that prefers manganese as a cofactor. *J Virol* **78**: 12218–12224. doi:10.1128/JVI.78.22.12218-12224.2004
- Bhardwaj K, Sun J, Holzenburg A, Guarino LA, Kao CC. 2006. RNA recognition and cleavage by the SARS coronavirus endoribonuclease. *J Mol Biol* **361**: 243–256. doi:10.1016/j.jmb.2006.06.021

- Bhardwaj K, Palaninathan S, Alcantara JMO, Li Yi L, Guarino L, Sacchetti JC, Kao CC. 2008. Structural and functional analyses of the severe acute respiratory syndrome coronavirus endoribonuclease Nsp15. *J Biol Chem* **283**: 3655–3664. doi:10.1074/jbc.M708375200
- Brogia L, Lecrivain AL, Renault TT, Hahnke K, Ahmed-Begrich R, Le Rhun A, Charpentier E. 2020. An RNA-seq based comparative approach reveals the transcriptome-wide interplay between 3'-to-5' exonucleases and RNase Y. *Nat Commun* **11**: 1587. doi:10.1038/s41467-020-15387-6
- Burge S, Parkinson GN, Hazel P, Todd AK, Neidle S. 2006. Quadruplex DNA: sequence, topology and structure. *Nucleic Acids Res* **34**: 5402–5415. doi:10.1093/nar/gkl655
- Cameron V, Uhlenbeck OC. 1977. 3'-phosphatase activity in T4 polynucleotide kinase. *Biochemistry* **16**: 5120–5126. doi:10.1021/bi00642a027
- Chen J, To L, de Mets F, Luo X, Majdalani N, Tai CH, Gottesman S. 2021. A fluorescence-based genetic screen reveals diverse mechanisms silencing small RNA signaling in *E. coli*. *Proc Natl Acad Sci* **118**: e2106964118. doi:10.1073/pnas.2106964118
- Choi JM, Park EY, Kim JH, Chang SK, Cho Y. 2004. Probing the functional importance of the hexameric ring structure of RNase PH. *J Biol Chem* **279**: 755–764. doi:10.1074/jbc.M309628200
- Condon C. 2010. What is the role of RNase J in mRNA turnover? *RNA Biol* **7**: 316–321. doi:10.4161/rna.7.3.11913
- Danielli L, Li X, Tuller T, Daniel R. 2020. Quantifying the distribution of protein oligomerization degree reflects cellular information capacity. *Sci Rep* **10**: 17689. doi:10.1038/s41598-020-74811-5
- Deutscher MP. 2009. Maturation and degradation of ribosomal RNA in bacteria. *Prog Mol Biol Transl Sci* **85**: 369–391. doi:10.1016/S0079-6603(08)00809-X
- Donovan WP, Kushner SR. 1986. Polynucleotide phosphorylase and ribonuclease II are required for cell viability and mRNA turnover in *Escherichia coli* K-12. *Proc Natl Acad Sci* **83**: 120–124. doi:10.1073/pnas.83.1.120
- Goodacre NF, Gerloff DL, Uetz P. 2013. Protein domains of unknown function are essential in bacteria. *MBio* **5**: e00744-13. doi:10.1128/mBio.00744-13
- Guarino LA, Bhardwaj K, Dong W, Sun J, Holzenburg A, Kao C. 2005. Mutational analysis of the SARS virus Nsp15 endoribonuclease: identification of residues affecting hexamer formation. *J Mol Biol* **353**: 1106–1117. doi:10.1016/j.jmb.2005.09.007
- Hackbart M, Deng X, Baker SC. 2020. Coronavirus endoribonuclease targets viral polyuridine sequences to evade activating host sensors. *Proc Natl Acad Sci* **117**: 8094–8103. doi:10.1073/pnas.1921485117
- Hor J, Matera G, Vogel J, Gottesman S, Storz G. 2020. Trans-acting small RNAs and their effects on gene expression in *Escherichia coli* and *Salmonella enterica*. *EcoSal Plus* **9**. doi:10.1128/ecosalplus.ESP-0030-2019
- Ishii R, Nureki O, Yokoyama S. 2003. Crystal structure of the tRNA processing enzyme RNase PH from *Aquifex aeolicus*. *J Biol Chem* **278**: 32397–32404. doi:10.1074/jbc.M300639200
- Ivanov KA, Hertzog T, Rozanov M, Bayer S, Thiel V, Gorbalenya AE, Ziebuhr J. 2004. Major genetic marker of nidoviruses encodes a replicative endoribonuclease. *Proc Natl Acad Sci* **101**: 12694–12699. doi:10.1073/pnas.0403127101
- Karimova G, Ullmann A, Ladant D. 2000. A bacterial two-hybrid system that exploits a cAMP signaling cascade in *Escherichia coli*. *Methods Enzymol* **328**: 59–73. doi:10.1016/S0076-6879(00)28390-0
- Kelley LA, Mezulis S, Yates CM, Wass MN, Sternberg MJ. 2015. The Phyre2 web portal for protein modeling, prediction and analysis. *Nat Protoc* **10**: 845–858. doi:10.1038/nprot.2015.053
- Laneve P, Altieri F, Fiori ME, Scaloni A, Bozzoni I, Caffarelli E. 2003. Purification, cloning, and characterization of XendoU, a novel endoribonuclease involved in processing of intron-encoded small nucleolar RNAs in *Xenopus laevis*. *J Biol Chem* **278**: 13026–13032. doi:10.1074/jbc.M211937200
- Lazarus MB, Novotny CJ, Shokat KM. 2015. Structure of the human autophagy initiating kinase ULK1 in complex with potent inhibitors. *ACS Chem Biol* **10**: 257–261. doi:10.1021/cb500835z
- Lehnik-Habrink M, Lewis RJ, Mader U, Stulke J. 2012. RNA degradation in *Bacillus subtilis*: an interplay of essential endo- and exoribonucleases. *Mol Microbiol* **84**: 1005–1017. doi:10.1111/j.1365-2958.2012.08072.x
- Liu B, Deikus G, Bree A, Durand S, Kearns DB, Bechhofer DH. 2014. Global analysis of mRNA decay intermediates in *Bacillus subtilis* wild-type and polynucleotide phosphorylase-deletion strains. *Mol Microbiol* **94**: 41–55. doi:10.1111/mmi.12748
- Liu B, Kearns DB, Bechhofer DH. 2016. Expression of multiple *Bacillus subtilis* genes is controlled by decay of *slrA* mRNA from Rho-dependent 3' ends. *Nucleic Acids Res* **44**: 3364–3372. doi:10.1093/nar/gkw069
- Mackie GA. 2013. RNase E: at the interface of bacterial RNA processing and decay. *Nat Rev Microbiol* **11**: 45–57. doi:10.1038/nrmicro2930
- Madeira F, Park YM, Lee J, Buso N, Gur T, Madhusoodanan N, Basutkar P, Tivey ARN, Potter SC, Finn RD, et al. 2019. The EMBL-EBI search and sequence analysis tools APIs in 2019. *Nucleic Acids Res* **47**: W636–W641. doi:10.1093/nar/gkz268
- Martins D, DiCandia MA, Mendes AL, Wetzel D, McBride SM, Henriques AO, Serrano M. 2021. CD25890, a conserved protein that modulates sporulation initiation in *Clostridioides difficile*. *Sci Rep* **11**: 7887. doi:10.1038/s41598-021-86878-9
- Mistry J, Chuguransky S, Williams L, Qureshi M, Salazar GA, Sonnhammer ELL, Tosatto SCE, Paladin L, Raj S, Richardson LJ, et al. 2021. Pfam: the protein families database in 2021. *Nucleic Acids Res* **49**: D412–D419. doi:10.1093/nar/gkaa913
- Nilsen TW. 2014. 3'-End labeling of RNA with [5'-³²P]cytidine 3',5'-bis(phosphate) and T4 RNA ligase 1. *Cold Spring Harb Protoc* **2014**: 444–446. doi:10.1101/pdb.prot080713
- Oussenko IA, Abe T, Ujiie H, Muto A, Bechhofer DH. 2005. Participation of 3'-to-5' exoribonucleases in the turnover of *Bacillus subtilis* mRNA. *J Bacteriol* **187**: 2758–2767. doi:10.1128/JB.187.8.2758-2767.2005
- Ricagno S, Egloff MP, Ulferts R, Coutard B, Nurizzo D, Campanacci V, Cambillau C, Ziebuhr J, Canard B. 2006. Crystal structure and mechanistic determinants of SARS coronavirus nonstructural protein 15 define an endoribonuclease family. *Proc Natl Acad Sci* **103**: 11892–11897. doi:10.1073/pnas.0601708103
- Rigden DJ. 2011. Ab initio modeling led annotation suggests nucleic acid binding function for many DUFs. *OMICS* **15**: 431–438. doi:10.1089/omi.2010.0122
- Rochat T, Delumeau O, Figueroa-Bossi N, Noirot P, Bossi L, Dervyn E, Boulloc P. 2015. Tracking the elusive function of *Bacillus subtilis* Hfq. *PLoS One* **10**: e0124977. doi:10.1371/journal.pone.0124977
- Saida F, Uzan M, Bontems F. 2003. The phage T4 restriction endoribonuclease RegB: a cyclizing enzyme that requires two histidines to be fully active. *Nucleic Acids Res* **31**: 2751–2758. doi:10.1093/nar/gkg377
- Soding J, Biegert A, Lupas AN. 2005. The HHpred interactive server for protein homology detection and structure prediction. *Nucleic Acids Res* **33**: W244–W248. doi:10.1093/nar/gki408
- Wang W, Bechhofer DH. 1996. Properties of a *Bacillus subtilis* polynucleotide phosphorylase deletion strain. *J Bacteriol* **178**: 2375–2382. doi:10.1128/jb.178.8.2375-2382.1996

Wen T, Oussenko IA, Pellegrini O, Bechhofer DH, Condon C. 2005. Ribonuclease PH plays a major role in the exonucleolytic maturation of CCA-containing tRNA precursors in *Bacillus subtilis*. *Nucleic Acids Res* **33**: 3636–3643. doi:10.1093/nar/gki675

Zhu B, Stulke J. 2018. SubtiWiki in 2018: from genes and proteins to functional network annotation of the model organism *Bacillus subtilis*. *Nucleic Acids Res* **46**: D743–D748. doi:10.1093/nar/gkx908

MEET THE FIRST AUTHOR



Shakti Ingle

Meet the First Author(s) is a new editorial feature within *RNA*, in which the first author(s) of research-based papers in each issue have the opportunity to introduce themselves and their work to readers of *RNA* and the *RNA* research community. Shakti Ingle is the first author of this paper, “Discovery and initial characterization of YloC, a novel endoribonuclease in *Bacillus subtilis*.” Shakti is a third-year postdoctoral fellow in the laboratory of David Bechhofer at the Icahn School of Medicine at Mount Sinai, New York, focusing on mRNA decay mechanisms in *B. subtilis*.

What are the major results described in your paper and how do they impact this branch of the field?

We discovered a novel endoribonuclease, encoded by the *yloc* gene, in *Bacillus subtilis* using classical protein biochemistry and mass spectrometry. YloC is a member of the YicC “family of proteins,” which is widespread in bacteria. RNA cleavage activity suggests YloC is a single-strand specific endoribonuclease with a preference for uridine residues. Structurally, YloC appears to form a hexamer, reminiscent of Nsp15 endoribonuclease of SARS coronaviruses. Although the precise biological role of YloC in *B. subtilis* remains to be discovered, we have shown by expressing YloC in *E. coli* that YloC may act to regulate the activity of small (sRNA) RNAs. Very little is known about the protein factors that impact sRNA regulation in *B. subtilis*. Conformation of the role of YloC in sRNA regulation will likely be a significant development for the study of this class of RNA in *B. subtilis*.

What led you to study RNA or this aspect of RNA science?

I studied inorganic chemistry for my MSc at Pune University and later for an MS at University of Cincinnati. I became interested in

RNA structure and dynamics after speaking with Professor Tom Tullius at Boston University and subsequently joined his laboratory as a graduate student. The idea of synthesizing modified (deuterated) nucleotides and incorporating them into RNA to study structure, using hydroxyl radical footprinting, intrigued me very much. This was the beginning of my research in RNA. For my postdoctoral studies, exploring the biological roles of RNA and RNA–protein interactions is my primary interest.

During the course of these experiments, were there any surprising results or particular difficulties that altered your thinking and subsequent focus?

A particular surprise in our study was when we discovered that YloC was, in fact, an endoribonuclease rather than a 3′ exoribonuclease, for which we had initially designed the RNase assay based on a 5′-IR800-labeled RNA.

Another interesting aspect of this work happened as we were contemplating the biological roles of YloC. Dr. Jiandong Chen’s research paper on YicC’s role in small RNA regulation in *E. coli* was published in bioRxiv (now in *PNAS*). This gave us a chance to collaborate with Dr. Chen and adopt the *E. coli* in vivo fluorescence assay to explore YloC function. In addition to being very productive, our collaboration has added significantly to the overall impact of this study.

Are there specific individuals or groups who have influenced your philosophy or approach to science?

Throughout my research training, several people have shaped my interest and approach in science. I would say that the approach to really question the data and to critically consider all aspects of the experimental design is something that has been impressed upon me in graduate school by my advisor, Dr. Tullius. I would like to add that this is very much also true about my current postdoctoral advisor, Dr. David Bechhofer.

What are your subsequent near- or long-term career plans?

We are pleased to see the recent discoveries of YloC and its homologs found to be important in biological processes in different bacterial species. Given the importance and prevalence of this protein, I am currently focusing on exploring the precise RNA cleavage specificity of YloC as well as its roles in small RNA regulation in *B. subtilis*. We are also pursuing avenues to solve the crystal structure of this interesting endoribonuclease. My long-term goal is to pursue a career in academics.